Original Article

The potential of indocyanine green fluorescence detection in surgical cut margin of breast conserving surgery

Hao Yu[1#], Yuhao Yao[2#], Tingting Zhu[3#], Yulu Sun[4], Meng Zhang[4], Yin Zhang[4], Meng Cao[4], Weijie Zhang[4], Yongzhong Yao[1,3,4]

[1]Division of Breast Surgery, Department of General Surgery, Nanjing Drum Tower Hospital, Nanjing Drum Tower Hospital Clinical College, Nanjing Medical University, Nanjing, China; [2]Department of Computer Science, Westcliff University, Irvine, CA, USA; [3]Division of Breast Surgery, Department of General Surgery, Nanjing Drum Tower Hospital, School of Medicine, Southeast University, Nanjing, China; [4]Division of Breast Surgery, Department of General Surgery, Nanjing Drum Tower Hospital, the Affiliated Hospital of Medical School, Nanjing University, Nanjing, China

Contributions: (I) Conception and design: Yongzhong Yao; (II) Administrative support: None; (III) Provision of study materials or patients: Y Zhang, W Zhang; (IV) Collection and assembly of data: H Yu, Yuhao Yao; (V) Data analysis and interpretation: T Zhu, M Zhang; (VI) Manuscript writing: All authors; (VII) Final approval of manuscript: All authors.

[#]These authors contributed equally to this work as co-first authors.

Correspondence to: Yongzhong Yao, MD, PhD. Division of Breast Surgery, Department of General Surgery, Nanjing Drum Tower Hospital, Nanjing Drum Tower Hospital Clinical College, Nanjing Medical University, Nanjing, China; Division of Breast Surgery, Department of General Surgery, Nanjing Drum Tower Hospital, School of Medicine, Southeast University, Nanjing, China; Division of Breast Surgery, Department of General Surgery, Nanjing Drum Tower Hospital, the Affiliated Hospital of Medical School, Nanjing University, 321 Zhongshan Road, Nanjing 210008, China. Email: yyh960508@Gmail.com.

Background: Fluorescence-guided surgery (FGS) is a cutting-edge technology that uses near-infrared (NIR) fluorescence imaging to guide surgeons in surgery. Indocyanine green (ICG) is a fluorescent dye, which can be used for *in vivo* imaging of tumor cells. We aimed to explore the use of ICG fluorescence-guided technology as a rapid intraoperative margin assessment method for breast cancer surgery. In addition, we also compared the dose selection of ICG.

Methods: This was a non-randomized prospective cohort study. Data were collected between August 2021 and October 2022 in the Division of Breast Surgery, Department of General Surgery, Nanjing Drum Tower Hospital, the Affiliated Hospital of Medical School, Nanjing University. Upon specimen removal, tumor margins were immediately analyzed by ICG fluorescence detection and then sent to the pathology department for intraoperative frozen section analysis and subsequent routine pathological examination. Abnormal margin rates were calculated and compared using intraoperative frozen section analysis and under the guidance of ICG fluorescence.

Results: The study included 69 cases of breast cancer patients who underwent tumor resection assisted by ICG fluorescence-guided technology, including 18 patients with a 0.5 mg/kg dose and 51 patients with a 1.0 mg/kg dose. According to the study findings, the ICG test achieved a sensitivity of 81.82% and a specificity of 75.82%. At a dose of 0.5 mg/kg, the sensitivity was 66.67% whereas the specificity was 93.33%. At the dose of 1 mg/kg, the sensitivity was 87.5%, and the specificity was 74.42%. Similarly, for intraoperative frozen section analysis, the sensitivity was 81.82%, but the specificity was enhanced to 94.83%. Positive surgical cut margin was not identified in 2/69 by ICG fluorescence and frozen section analysis respectively.

Conclusions: The sensitivity of ICG fluorescence detection is comparable to that of frozen section analysis, but the specificity is poor. The sensitivity increased and the specificity decreased at 1 mg/kg compared to the 0.5 mg/kg dose. ICG fluorescence can be used as a supplementary tool for frozen section analysis. These findings support further development and clinical performance assessment of ICG fluorescence.

Keywords: Near-infrared fluorescence (NIF); fluorescence-guided surgery (FGS); indocyanine green (ICG); breast-conserving surgery (BCS); surgical safety margin

Submitted May 27, 2024. Accepted for publication Jun 24, 2024. Published online Jun 27, 2024.
doi: 10.21037/gs-24-195
View this article at: https://dx.doi.org/10.21037/gs-24-195

Introduction

Breast cancer has the highest incidence rate among women worldwide and is the most common form of malignancy among all cancers. Each year, an estimated 2.3 million new cases (11.7%) and 700,000 deaths (6.9%) are attributed to breast cancer (1,2). Despite the growing range of treatment options available for breast cancer, surgery remains an important aspect of early-stage treatment (3). Breast-conserving surgery (BCS) is considered a minimally invasive surgical procedure that aims to remove the tumor while preserving the breast tissue. Although BCS minimizes the physical and psychological morbidity for patients, achieving clear surgical margins is crucial to reduce the risk of local recurrence (4). Positive margins triple the risk of ipsilateral recurrence and may be responsible for 75% of local recurrences and metastases (5-7).

Currently, intraoperative margin assessment predominantly relies on surgeons' visual and tactile judgment, followed by frozen section analysis for confirmation (8-10). However, frozen section analysis also has several disadvantages—it is time-consuming and labor-intensive, and requires skilled professionals for processing (11). Therefore, researchers are searching for other sensitive and convenient methods to reduce the positive surgical margin rate.

Fluorescence-guided surgery (FGS) is an innovative technique that uses fluorescent agents to improve surgical outcomes by enhancing intraoperative visualization of desired tissues and structures. By labelling certain tissues or structures with a fluorescent dye, the surgeon is able to visualize and distinguish them more easily during a surgical procedure (12). It shows great potential in cardiac surgery, oncological surgery, or neurosurgery (13,14). Indocyanine green (ICG) is a water-soluble tricarbocyanine dye that can be detected by near-infrared fluorescence (NIF) imaging equipment. Its use in the assessment of cardiac and hepatic function, retinal imaging, and choroidal vasculopathy is well documented (15). In recent years, ICG has also been used to locate lymph nodes, such as in stomach (16-18), as well as for surgical localization of sites and metastases involving the tumor (19-21). The purpose of this study was to investigate whether ICG fluorescence can be used as a supplementary tool for frozen section analysis. In this study, we evaluated the value of different doses of ICG in determining surgical margins by injecting 0.5 mg/kg of ICG the morning before surgery and 1 mg/kg of ICG on the night before surgery. We present this article in accordance with the STROBE reporting checklist (available at https://gs.amegroups.com/article/view/10.21037/gs-24-195/rc).

Highlight box

Key findings

- Indocyanine green (ICG) fluorescence tracing can be used as a supplementary tool for frozen section analysis, with high sensitivity and very short assessment time.

What is known and what is new?

- Positive margins are associated with an increased risk of breast cancer recurrence. Frozen section analysis is the main option for diagnosing positive margins, but it is time consuming and laborious.
- In this study, ICG fluorescence detection of cancer margins in 69 breast-conserving operations showed high sensitivity in a short period of time. The dose of 1 mg/kg increased sensitivity and decreased specificity of detection compared to the dose of 0.5 mg/kg.

What is the implication, and what should change now?

- ICG fluorescence can be used as a supplementary tool for frozen section analysis. These findings support further development and clinical performance assessment of ICG fluorescence.

Methods

Study methods

A non-randomized prospective cohort study was conducted. According to previous literature, the fluorescence visualization rate of ICG on tumor tissue is 0.893 and its 95% confidence interval is 0.808–0.978. Using the target value of 80.9%, a unilateral test level of 0.025, and a test efficacy of 80%, the sample size of the current study was calculated to be at least 51 cases (12,15). Taking into

account the possibility of test shedding, 60 samples were expected to be included in this study. Eventually, based on the inclusion and exclusion criteria, 69 patients with early-stage breast cancer who underwent BCS in the Division of Breast Surgery, Department of General Surgery, Nanjing Drum Tower Hospital, the Affiliated Hospital of Medical School, Nanjing University from August 2021 to October 2022 were selected.

The inclusion criteria were patients aged 18–75 years with breast cancer who were eligible for BCS. Exclusion criteria were inflammatory breast cancer, previous allergy to ICG and iodine, cardiovascular and cerebrovascular disease, significant organ damage, and inability to tolerate surgery. The study was conducted in accordance with the Declaration of Helsinki (as revised in 2013). The study was approved by the Ethics Committee of Nanjing Drum Tower Hospital (No. 2020-024) and informed consent was taken from all the patients.

Surgery

Participants who met the inclusion criteria received ICG dissolved in sterile water at a dose of 0.5 or 1 mg/kg according to body weight mixed in 100 mL dextrose solution before surgery, and the infusion was completed by peripheral intravenous drip for 30 minutes. Patients received an injection of 0.5 mg/kg ICG at 6:00 on the day prior to surgery or 1 mg/kg ICG at 20:00 on the first day before surgery. The patient's vital signs were closely monitored.

All surgeries in this trial were performed by senior consultants. The surgeries were performed according to the BCS procedure for breast cancer. After the specimen was removed from the body, the NIF imaging device called FLI-10B (Nanjing Nuoyuan Medical Devices, Co., Ltd., Nanjing, China) was used to image 30–40 cm above the patient's primary tumor sites and the surrounding surgical field in accordance with the requirements of the Fluorescence Image Navigation System clinical trial programme. If an incisal margin is considered positive after NIF detection, supplementary excision is performed at the patient's surgical site corresponding to the "positive" margin. The supplementary margin will be detected again by NIF detection. The images were captured under optimal lighting conditions in the operating room, using automatic exposure settings. Each side of the specimen was positioned and photographed according to preset parameters. The NIF detection was performed after completion of the examination, with specimens sent to frozen section analysis for detection after examination. Highlighted areas were individually labelled and sent for frozen section analysis. The specimen was selected from the lesion site. OCT embedding medium was applied, and the specimen was rapidly frozen at –20 ℃ for 3 minutes. The section thickness was maintained at 5–6 μm, and the sections were fixed in a 10% formalin solution, subjected to hematoxylin and eosin (HE) staining, mounted with rhamsan gum and evaluated by pathologists. All surgical specimens were followed by routine pathological examination, and the final status of the margins was determined according to the postoperative pathological results. All pathologies were analyzed by two experienced senior pathologists.

Quantitative analysis of fluorescence imaging

During the procedure, fluorescence measurements were taken using the FLI-10B instrument (Nanjing Nuoyuan Medical Devices, Co., Ltd.). The device has a color scale analysis system that can be quantitatively analyzed. During the procedure, the FLI-10B instrument's built-in software was used to measure the fluorescence values on the specimen surface and the adjacent breast tissue, which was considered the 'background'. Finally, the surface-to-background fluorescence ratio (SBR) was calculated for each specimen. We defined SBR >1.5 is the cut off value.

Medicines

ICG for injection, specification: 25 mg, manufacturer: Dandong Medical Chuang Pharmaceutical Co., Ltd. (Donggang, China), storage conditions: shielded from light, airtight, stored in a cold place (2–10 ℃). Glucose injection, specification: 100 mL, manufacturer: Otsuka (Zhangjiagang, China).

Statistical analysis

Quantitative variables were described by mean ± standard deviation (normal distribution) or median ± interquartile spacing (non-normal distribution). Categorical variables were described as numbers and proportions. For between-group comparisons, one-way analysis of variance (ANOVA) was used for analyses of continuous variables conforming to a normal distribution, the Kruskal-Wallis test for analyses of continuous non-normally distributed or hierarchical data, and Pearson's chi-square test or Fisher's exact test

for analyses of categorical variables, with post hoc tests if significant P values were available (Bonferroni test) to determine where the differences were located. Kappa coefficient was used to assess the internal consistency and reliability of the measurement tools used in this study. The results of Kappa coefficient were classified as slight (0.0 to 0.20), fair (0.21 to 0.40), moderate (0.41 to 0.60), and substantial (0.61 to 0.80) and almost perfect (0.81 to 1). All analyses were performed under good clinical practice standards using IBM SPSS Statistics for Windows, Version 25.0 (IBM Corp., Armonk, NY, USA).

Results

From August 2021 to October 2022, a total of 73 patients were recruited to the study. After excluding 3 patients due to loss of imaging data, a total of 69 patients were finally enrolled in the study. Patients received an injection of 0.5 mg/kg ICG at 6:00 on the day prior to surgery or 1 mg/kg ICG at 20:00 on the first day before surgery. Routine pathological examination of surgical margins was positive in 11 out of 69 patients. The NIF detection and frozen sections analysis detected 9 positive surgical margins respectively. At a dose of 0.5 mg/kg, NIF detected a positive incisal margin in 2/3 of cases, and at a dose of 1 mg/kg, NIF detected a positive incisal margin in 7/8 cases. Patient and tumor characteristics are shown in *Table 1*. Some of the indicators that may be relevant to the outcome are analyzed in *Table 2*. According to the effects of different doses, we conducted a separate analysis in *Table 3*. At the dose of 0.5 mg/kg, tumor grade, histologic type, and tumor size may affect the results of NIF detection. We cannot rule out this is due to the small sample size. No statistically significant factors were found at the dose of 1 mg/kg.

After removal of the mammary segment, we bisected the isolated specimens and placed it under the FLI-10B. It could be clearly seen that the fluorescence intensity gradually decreased from the center of the tumor to the surrounding, showing that the concentration of ICG in

Table 1 Patient demographics and clinical information

Characteristics	All (n=69)	0.5 mg/kg (n=18)	1.0 mg/kg (n=51)	P value
Injection time (h)	12.63±6.03	4.30±1.81	15.57±3.80	0.06
BMI (kg/m^2)				0.99
<24	38 (55.1)	11 (61.1)	27 (52.9)	
≥24	31 (44.9)	7 (38.9)	24 (47.1)	
Tumor quadrant				0.57
UOQ	16 (23.2)	4 (22.2)	12 (23.5)	
OQT	9 (13.0)	1 (5.5)	8 (15.7)	
LOQ	14 (20.3)	4 (22.2)	10 (19.6)	
LQT	4 (5.8)	0 (0.0)	4 (7.8)	
LIQ	5 (7.2)	1 (5.5)	4 (7.8)	
IQT	0 (0.0)	0 (0.0)	0 (0.0)	
UIT	11 (15.9)	3 (16.7)	8 (15.7)	
UQT	10 (14.5)	5 (27.8)	5 (9.8)	
Histologic type				0.37
IDC	56 (81.2)	14 (77.8)	42 (82.4)	
ILC	3 (4.3)	2 (11.1)	1 (2.0)	
Carcinoma *in situ*	2 (2.9)	0 (0.0)	2 (3.9)	
Other types	8 (11.6)	2 (11.1)	6 (11.8)	

Table 1 *(continued)*

Table 1 *(continued)*

Characteristics	All (n=69)	0.5 mg/kg (n=18)	1.0 mg/kg (n=51)	P value
T				0.06
Tis	2 (2.9)	0 (0.0)	2 (3.9)	
T1	35 (50.7)	14 (77.8)	21 (41.2)	
T2	31 (44.9)	4 (22.2)	27 (52.9)	
T3	1 (1.4)	0(0.0)	1 (2.0)	
N				0.65
N0	53 (76.8)	16 (88.9)	37 (72.5)	
N1	13 (18.8)	2 (11.1)	11 (21.6)	
N2	2 (2.9)	0 (0.0)	2 (3.9)	
N3	1 (1.4)	0 (0.0)	1 (2.0)	
Tumor grade*				0.32
I	12 (17.4)	4 (22.2)	8 (15.7)	
II	35 (50.7)	10 (55.6)	25 (49.0)	
III	17 (24.6)	2 (11.1)	15 (29.4)	
Carcinoma *in situ* components				<0.001
Yes	53 (76.8)	8 (44.4)	45 (88.2)	
No	16 (23.2)	10 (55.6)	6 (11.8)	
Vascular invasion*				>0.99
Yes	13 (18.8)	3 (16.7)	10 (19.6)	
No	54 (78.3)	15 (83.3)	39 (76.5)	
Neural invasion*				0.10
Yes	8 (11.9)	0 (0.0)	8 (15.7)	
No	59 (88.1)	18 (100.0)	41 (80.4)	
Molecular typing*				0.70
$HR^+/HER2^-$	49 (71.0)	13 (72.2)	36 (70.6)	
$HR^+/HER2^+$	5 (7.2)	2 (11.1)	3 (5.9)	
Basal-like	10 (14.5)	2 (11.8)	8 (15.7)	
$HR^-/HER2^+$	2 (2.9)	0 (0.0)	2 (3.9)	

Quantitative variables were described by mean ± standard deviation. Categorical variables were described as n (%). Group differences were compared using the ANOVA. Percentage totals may not add to 100% due to rounding. *, 2 cases of carcinoma *in situ* were not included in tumor grade, vascular invasion, neural invasion and molecular typing. One case of papillary carcinoma and 1 case of invasive carcinoma <0.1 cm were not included in tumor grade and molecular typing. One case of invasive carcinoma =0.1 cm was not included in tumor grade. BMI, body mass index; UOQ, upper outer quadrant; OQT, outer quadrant transition; LOQ, lower outer quadrant; LQT, lower quadrant transition; LIQ, lower inner quadrant; IQT, inner quadrant transition; UIT, upper inner transition; UQT, upper quadrant transition; IDC, invasive ductal carcinoma; ILC, invasive lobular carcinoma; HR, hormone receptor; HER2, human epidermal growth factor 2; ANOVA, one-way analysis of variance.

Table 2 Indicators of possible relevance to fluorescent tracers

Characteristics	Success (n=55)	Failure (n=14)	P value
Age (years)	51.16±9.54	54.21±12.32	0.32
BMI (kg/m^2)	23.87±3.57	25.18±4.15	0.24
<24	35 (63.6)	3 (21.4)	
≥24	20 (36.4)	11 (78.6)	
Tumor quadrant			0.88
UOQ	14 (25.5)	2 (14.2)	
OQT	6 (10.9)	3 (21.4)	
LOQ	10 (18.2)	4 (28.6)	
LQT	4 (7.3)	0 (0.0)	
LIQ	5 (9.1)	0 (0.0)	
IQT	0 (0.0)	0 (0.0)	
UIT	8 (14.5)	3 (21.4)	
UQT	8 (14.5)	2 (14.2)	
Tumor grade*			0.31
I	11 (20.0)	1 (7.1)	
II	28 (50.9)	7 (50.0)	
III	12 (21.8)	5 (35.7)	
Histologic type			0.86
IDC	45 (81.8)	11 (78.6)	
ILC	3 (5.5)	0 (0.0)	
CIS	2 (3.6)	0 (0.0)	
Other	5 (9.1)	3 (21.4)	
T			0.24
Tis	2 (3.6)	0 (0.0)	
T1	25 (45.5)	10 (71.4)	
T2	27 (49.1)	4 (28.6)	
T3	1 (1.8)	0 (0.0)	
N			0.98
N0	43 (78.2)	10 (71.4)	
N1	9 (16.4)	4 (28.6)	
N2	2 (3.6)	0 (0.0)	
N3	1 (1.8)	0 (0.0)	
Carcinoma *in situ* components			0.49
Yes	42 (76.4)	11 (78.6)	
No	13 (23.6)	3 (21.4)	
Vascular invasion*			0.66
Yes	11 (20.0)	2 (14.2)	
No	42 (76.4)	12 (85.7)	
Neural invasion*			0.57
Yes	6 (10.9)	2 (14.2)	
No	47 (85.5)	12 (85.7)	
Molecular typing*			0.49
HR$^+$/HER2$^-$	39 (70.9)	10 (71.4)	
HR$^+$/HER2$^+$	5 (9.1)	0 (0.0)	
Basal-like	7 (12.7)	3 (21.4)	
HR$^-$/HER2$^+$	2 (3.6)	0 (0.0)	
ICG dose (mg/kg)			0.66
0.5	16 (29.1)	2 (14.2)	
1	39 (70.9)	12 (85.7)	

Quantitative variables were described by mean ± standard deviation. Categorical variables were described as n (%). Group differences were compared using the ANOVA. Percentage totals may not add to 100% due to rounding. *, 2 cases of carcinoma *in situ* were not included in tumor grade, vascular invasion, neural invasion and molecular typing. One case of papillary carcinoma and 1 case of invasive carcinoma <0.1 cm were not included in tumor grade and molecular typing. One case of invasive carcinoma =0.1 cm was not included in tumor grade. BMI, body mass index; UOQ, upper outer quadrant; OQT, outer quadrant transition; LOQ, lower outer quadrant; LQT, lower quadrant transition; LIQ, lower inner quadrant; IQT, inner quadrant transition; UIT, upper inner transition; UQT, upper quadrant transition; IDC, invasive ductal carcinoma; ILC, invasive lobular carcinoma; CIS, carcinoma in situ; HR, hormone receptor; HER2, human epidermal growth factor 2; ICG, indocyanine green; ANOVA, one-way analysis of variance.

the tumor was much higher than that in the normal tissue (*Figure 1*).

A special case showed abnormal fluorescence images at the surgical cut margin (*Figure 2A*). The frozen section analysis of this sample did not reveal tumor at the surgical cut margin, while NIF detected high light fluorescence. After a supplementary resection, an intraoperative frozen section analysis was performed. The frozen section analysis showed the supplementary margin was negative, but routine pathology revealed a carcinoma *in situ* component 0.7 mm from the margin (*Figure 2B*).

Table 3 Indicators of possible relevance to fluorescent tracers at a dose of 0.5 and 1 mg/kg

Characteristics	0.5 mg/kg			1 mg/kg		
	Success (n=16)	Failure (n=2)	P value	Success (n=39)	Failure (n=12)	P value
Age (years)	55.56±8.99	56.50±10.6	0.88	58.69±2.05	67.94±9.14	0.53
BMI (kg/m^2)	23.95±4.73	22.45±22.45	0.49	23.53±3.19	26.73±2.96	0.71
<24	10 (62.5)	1 (50.0)		25 (64.1)	2 (16.7)	
≥24	6 (37.5)	1 (50.0)		14 (35.9)	10 (83.3)	
Tumor quadrant			0.80			0.60
UOQ	4 (25.0)	0 (0.0)		10 (25.6)	2 (16.7)	
OQT	1 (6.3)	0 (0.0)		5 (12.8)	3 (25.0)	
LOQ	3 (18.8)	1 (50.0)		7 (17.9)	3 (25.0)	
LQT	0 (0.0)	0 (0.0)		4 (10.3)	0 (0.0)	
LIQ	1 (6.3)	0 (0.0)		4 (10.3)	0 (0.0)	
IQT	0 (0.0)	0 (0.0)		0 (0.0)	0 (0.0)	
UIT	3 (18.8)	0 (0.0)		5 (12.8)	3 (25.0)	
UQT	4 (25.0)	1 (50.0)		4 (10.3)	1 (8.3)	
Tumor grade*			0.04			0.76
I	3 (18.8)	1 (50.0)		7 (17.9)	1 (8.3)	
II	10 (62.5)	0 (0.0)		18 (46.2)	7 (58.3)	
III	1 (6.3)	1 (50.0)		11 (28.2)	4 (33.3)	
Histologic type			0.04			0.61
IDC	13 (81.3)	1 (50.0)		32 (82.1)	10 (83.3)	
ILC	2 (12.5)	0 (0.0)		1 (2.6)	0 (0.0)	
CIS	0 (0.0)	0 (0.0)		2 (5.1)	0 (0.0)	
Other	1 (6.3)	1 (50.0)		4 (10.3)	2 (16.7)	
T			0.04			0.22
Tis	0 (0.0)	0 (0.0)		2 (5.1)	0 (0.0)	
T1	12 (75.0)	2 (100.0)		13 (33.3)	8 (66.7)	
T2	4 (25.0)	0 (0.0)		23 (59.0)	4 (33.3)	
T3	0 (0.0)	0 (0.0)		1 (2.6)	0 (0.0)	
N			0.26			0.51
N0	14 (87.5)	2 (100.0)		29 (74.4)	8 (66.7)	
N1	2 (12.5)	0 (0.0)		7 (17.9)	4 (33.3)	
N2	0 (0.0)	0 (0.0)		2 (5.1)	0 (0.0)	
N3	0 (0.0)	0 (0.0)		1 (2.6)	0 (0.0)	
Carcinoma *in situ* components			0.87			0.26
Yes	7 (43.8)	1 (50.0)		35 (90.0)	10 (83.3)	
No	9 (56.3)	1 (50.0)		4 (10.3)	2 (16.7)	

Table 3 *(continued)*

Table 3 *(continued)*

Characteristics	0.5 mg/kg			1 mg/kg		
	Success (n=16)	Failure (n=2)	P value	Success (n=39)	Failure (n=12)	P value
Vascular invasion*			0.12			0.55
Yes	3 (18.8)	0 (0.0)		8 (20.5)	2 (16.7)	
No	13 (81.3)	2 (100.0)		29 (74.4)	10 (83.3)	
Neural invasion*			–			0.55
Yes	0 (0.0)	0 (0.0)		6 (15.4)	2 (16.7)	
No	16 (100.0)	2 (100.0)		31 (79.5)	10 (83.3)	
Molecular typing*			–			0.002
$HR^+/HER2^-$	13 (81.3)	0 (0.0)		26 (66.7)	10 (83.3)	
$HR^+/HER2^+$	2 (12.5)	0 (0.0)		3 (7.7)	0 (0.0)	
Basal-like	1 (62.5)	1 (50.0)		6 (15.4)	2 (16.7)	
$HR^-/HER2^+$	0 (0.0)	0 (0.0)		2 (5.1)	0 (0.0)	

Quantitative variables were described by mean ± standard deviation. Categorical variables were described as numbers and proportions. Group differences were compared using the ANOVA. Percentage totals may not add to 100% due to rounding. *, 2 cases of carcinoma *in situ* were not included in tumor grade, vascular invasion, neural invasion and molecular typing. One case of papillary carcinoma and 1 case of invasive carcinoma <0.1 cm were not included in tumor grade and molecular typing. One case of invasive carcinoma =0.1 cm was not included in tumor grade. BMI, body mass index; UOQ, upper outer quadrant; OQT, outer quadrant transition; LOQ, lower outer quadrant; LQT, lower quadrant transition; LIQ, lower inner quadrant; IQT, inner quadrant transition; UIT, upper inner transition; UQT, upper quadrant transition; IDC, invasive ductal carcinoma; ILC, invasive lobular carcinoma; CIS, carcinoma in situ; HR, hormone receptor; HER2, human epidermal growth factor 2; ANOVA, one-way analysis of variance.

SBR >1.5 is the cut off value of this study. NIF detection groups refer to the detection of the primary tumor site and surrounding area by FLI-10B above 30–40 cm after the specimen has been isolated from the patient. Frozen section analysis groups refer to the analysis of sections of tissue by pathologists through freezing techniques. The true positive (TP) rate for NIF detection was 81.82%, whereas the true negative (TN) rate was 79.31%. The positive predictive value (PPV) was 42.85%, and the negative predictive value (NPV) was 95.83%. Frozen section analysis provided a TP rate of 81.82% and a TN rate of 98.28%, with a PPV of 90% and an NPV of 96.61% (*Table 4*). At a dose of 0.5 mg/kg, the TP rate was 66.67% whereas the TN rate was 93.33%. At the dose of 1 mg/kg, the TP rate was 87.5%, and the TN was 74.42%. Specifically, the NPV of NIF detection at 0.5 mg/kg dose was 93.33% and that of NIF detection at 1 mg/kg dose was 96.97% (*Table 5*). When calculating the sensitivity and specificity of different concentrations of ICG, it was discovered that the dose of 1 mg/kg increased the sensitivity of NIF detection compared to the dose of 0.5 mg/kg, but at the same time reduced its specificity. The Kappa coefficient for ICG and routine pathological tests was 0.447, while that for 0.5 mg/kg was 0.600, and for 1 mg/kg was 0.410, all indicating moderate consistency.

Discussion

Thanks to the advances in screening and examination techniques, breast cancer detection rates have steadily increased and the majority of breast cancers can now be detected at an early stage (22). BCS is a surgical procedure aimed at removing tumor lesions while preserving breast tissue. BCS aids in maintaining the patient's physical and mental wellbeing, as well as promoting the appearance of their breast, when compared to radical mastectomy (23-25). However, BCS needs to ensure that the margin is negative to prevent recurrence (26). In addition to pathological methods, some new methods are also being studied, such as genetic testing, imaging evaluation, and optically- or artificial intelligence-assisted prediction models (27,28).

The main purpose of this study was to evaluate the accuracy of intraoperative NIF imaging in removing tumors

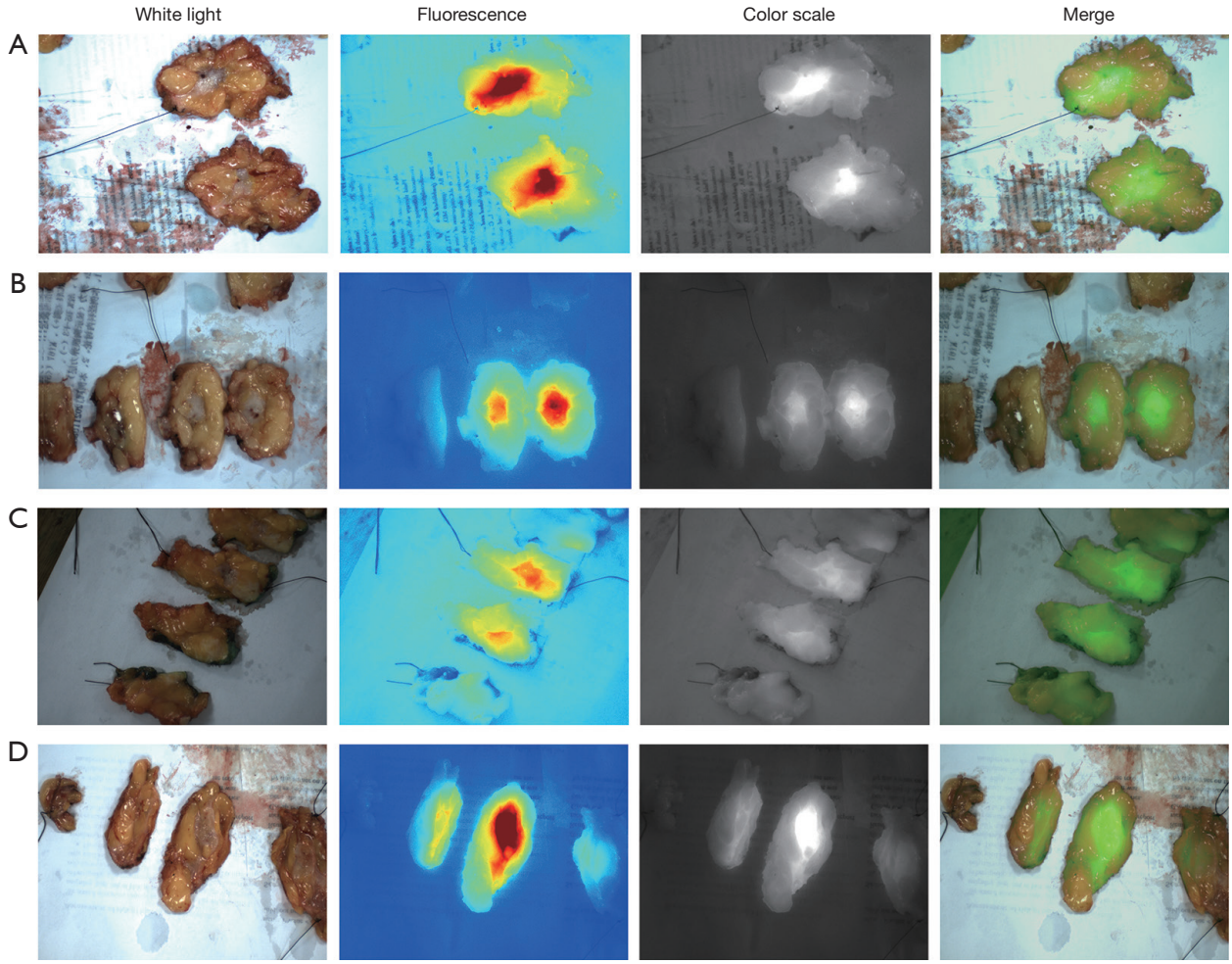

Figure 1 Fluorescence of dissected tumor. NIF detection of isolated tumors in white light, fluorescence, color scale and merger modes. ICG can be found accumulating in the tumor tissue after sectioning the specimen, which is different from the paracancerous tissue. (A) Patient was injected 4 hours prior to surgery at a dose of 0.5 mg/kg. The tumor size was 1.5 cm. (B) Patient was injected 3 hours prior to surgery at a dose of 0.5 mg/kg with a tumor size of 1.8 cm. (C) Patient was injected 8 hours prior to surgery at a dose of 1 mg/kg with a tumor size of 2.3 cm. (D) Patient was injected 2 hours prior to surgery at a dose of 0.5 mg/kg with a tumor size of 1.9 cm. NIF, near-infrared fluorescence; ICG, indocyanine green.

of BCS. Conventional pathology showed that the final NIF NPV was 95.83%, which was slightly lower than the NPV of intraoperative frozen section analysis (98.28%). This result shows that intraoperative NIF imaging has certain potential in rapid identification of negative margins. Moreover, we have also increased our understanding of the effects of ICG at different time points and doses on tumor detection. This is crucial for the implementation of the technology and the interpretation of the results in future research.

Intraoperative frozen section analysis is a more accurate detection method and a key tool for BCS (9). However, it has disadvantages such as being time-consuming and labor-intensive (11,29). Previous studies have shown that the use of ICG can be used to identify tumors and normal tissues in colon cancers (30). ICG has been used to identify the surgical margins of gastrointestinal tumors, lung cancer, and so on (31-33). In breast cancer surgery, ICG has also been tried for tumor localization or margin determination with satisfactory results (34-36). At the same time, due to the existence of some special types of tumors in breast cancer, such as invasive micropapillary carcinoma, ductal carcinoma

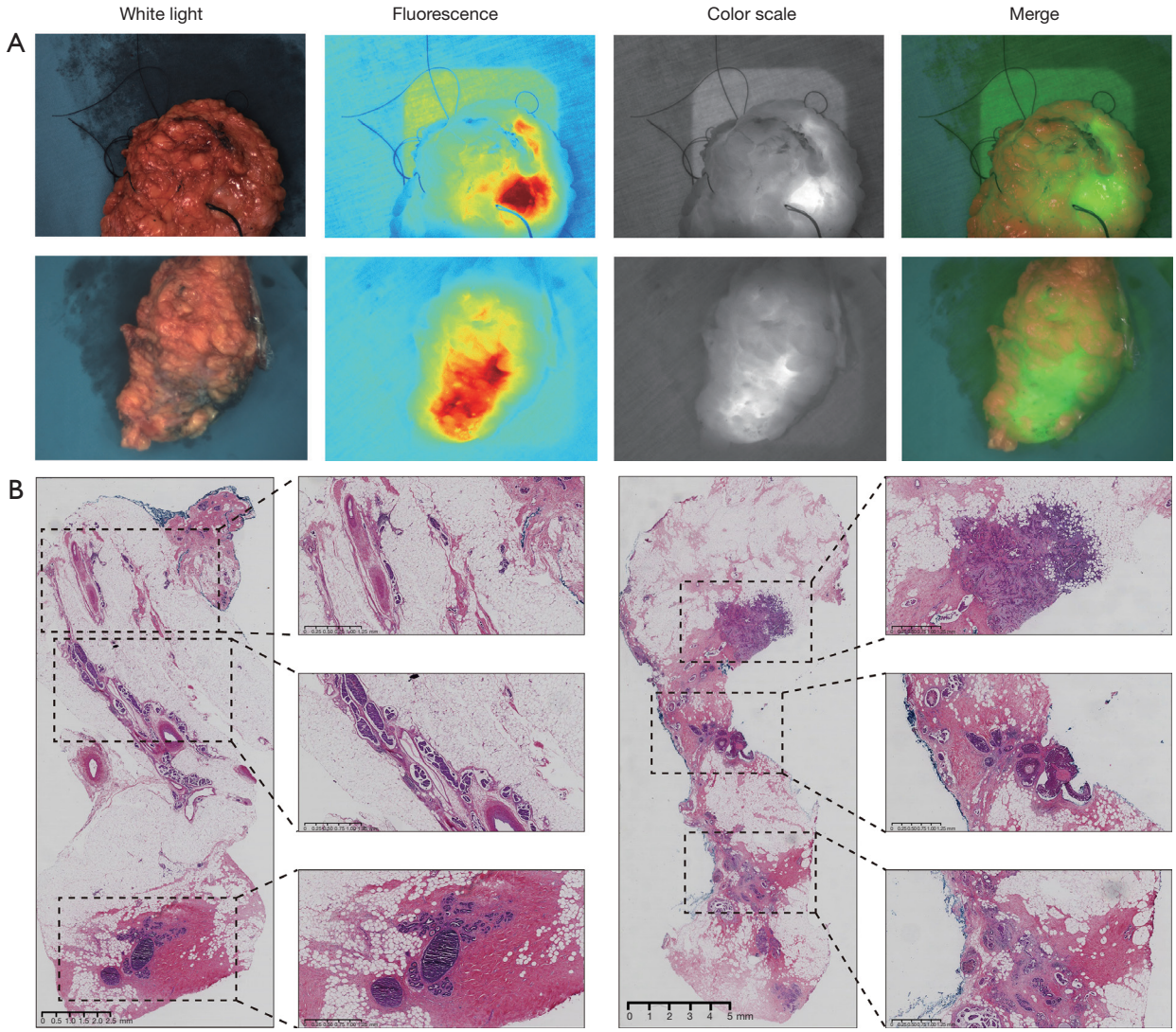

Figure 2 Tumor specimens with positive margin. (A) Example of an *ex vivo* (after resection) whole specimen, abnormal fluorescence images were observed at the surgical cut margin and identified as residual tumor tissue. (B) Hematoxylin and eosin stains are used to determine tumor cells from normal cells. Postoperative pathology showed a carcinoma *in situ* component 0.7 mm from the margins whereas frozen biopsy margins showed no tumor tissue.

Table 4 Sensitivity and specificity by NIF detection and frozen section analysis

Detection result		Routine pathological examination			Accuracy		
		Positive	Negative	Total	TP (%)	TN (%)	NPV (%)
NIF detection	Positive	9	12	21	81.82	79.31	95.83
	Negative	2	46	48			
Frozen section analysis	Positive	9	1	10	81.82	98.28	96.61
	Negative	2	57	59			

NIF, near-infrared fluorescence; TP, true positive; TN, true negative; NPV, negative predictive value.

Table 5 Sensitivity and specificity by NIF detection of 0.5 and 1 mg/kg

Detection result		Routine pathological examination			Accuracy		
		Positive	Negative	Total	TP (%)	TN (%)	NPV (%)
NIF detection at a dose of 0.5 mg/kg	Positive	2	1	3	66.67	93.33	93.33
	Negative	1	14	15			
NIF detection at a dose of 1 mg/kg	Positive	7	11	18	87.5	74.42	96.97
	Negative	1	32	33			

NIF, near-infrared fluorescence; TP, true positive; TN, true negative; NPV, negative predictive value.

in situ, etc., it is difficult to identify the surgical margin (37,38). Therefore, this study explored the identification of surgical cut margin of BCS to find a more effective means of detection. During the operation, we removed the tumor completely and cut it. It could be clearly seen that the fluorescence intensity gradually decreases from the center of the tumor to the surrounding, which shows that ICG can specifically accumulate in the tumor tissue. Due to the characteristics of frozen sections, it is more difficult to identify the components of carcinoma *in situ* than those of invasive carcinoma for most breast cancers (39). Residual tumor is an important cause of postoperative recurrence (22,40). Among the 69 patients, 2 cases of frozen section analysis failed to identify positive surgical cut margin. One case was *in situ* carcinoma 0.7 mm away from the surgical cut margin, and the other case was 1 mm away from the surgical cut margin, and ICG was identified as positive surgical cut margin. A special case showed the first frozen section analysis failed to identify the positive surgical cut margin during the operation while NIF found the positive fluorescence. We performed an extended excision at the location of the margin during surgery. The second frozen section analysis showed that the margin was positive, and the total resection was finally selected. Similarly, frozen section analysis failed to detect positive incisal margins in two patients' surgical cut margin, including 1 case of carcinoma *in situ* from the nearest margin of 0.2 mm, and the other case of carcinoma *in situ* from the nearest margin of <0.5 mm, and intraoperative frozen section analysis showed positive outcome. Therefore, ICG shows potential in the choice of surgical methods and prognosis of patients during surgery, which can be combined with frozen section analysis to reduce the possibility of secondary trauma and provide help for treatment.

In terms of ICG dose selection, we initially tried to use a dose of 0.5 mg/kg to conduct experiments around 6 hours before surgery, but this time point tends to be in the early hours of the morning, which has a certain impact on the conduction of the experiment. Therefore, the subsequent change to a dose of 1 mg/kg was carried out around 14 hours before surgery. The results showed that the sensitivity increased and the specificity decreased at 1 mg/kg compared to the 0.5 mg/kg dose. All patients had no adverse reactions after injection. Although the number of patients is small, we can still see the relationship between ICG dose and recognition rate, which will also provide help for subsequent research.

In this study, one patient's data were excluded due to environmental factors, and two patients' data were incomplete. This issue was caused by operator error, which can be rectified with simple training. In comparison to the extensive professional training required for frozen section analysis, the diagnostic aspect of NIF surgery is significantly less demanding, which is a substantial advantage.

There are some limitations in this study. Firstly, the sample size was insufficient to fully validate the reliability of BCS margin recognition using ICG Fluorescence detection. Secondly, although fluorescence can be quantified using machines, determining whether the margin is positive still requires subjective judgment, which might lead to confounding variables.

Although there are several limitations, the findings of this study demonstrate that ICG fluorescence detection can function as a supplementary tool to efficiently detect positive surgical cut margin. It can be applied in BCS for breast cancer, offering a novel approach to detect surgical margins whilst presenting a favorable clinical outlook.

Conclusions

The findings of the validation presented here suggest that ICG could be useful for surgical cut margin in BCS,

particularly in terms of sensitivity similar to frozen section analysis. ICG can detect cancerous tissue not identified by frozen section analysis. The sensitivity increased and the specificity decreased at 1 mg/kg compared to the 0.5 mg/kg dose. ICG fluorescence can be used as a supplementary tool for frozen section analysis.

Although the results are encouraging for ICG, more trials are needed to investigate whether the current experimental protocols can positively impact intra-operative decision making and patient prognosis.

Acknowledgments

The authors are grateful to the Nanjing Nuoyuan Medical Devices, Co., Ltd. for providing products.
Funding: This study was supported by the Medical Science and Technology Development Foundation, Nanjing Department of Health (No. ZKX20025).

Footnote

Reporting Checklist: The authors have completed the STROBE reporting checklist. Available at https://gs.amegroups.com/article/view/10.21037/gs-24-195/rc

Data Sharing Statement: Available at https://gs.amegroups.com/article/view/10.21037/gs-24-195/dss

Peer Review File: Available at https://gs.amegroups.com/article/view/10.21037/gs-24-195/prf

Conflicts of Interest: All authors have completed the ICMJE uniform disclosure form (available at https://gs.amegroups.com/article/view/10.21037/gs-24-195/coif). The authors have no conflicts of interest to declare.

Ethical Statement: The authors are accountable for all aspects of the work in ensuring that questions related to the accuracy or integrity of any part of the work are appropriately investigated and resolved. The study was conducted in accordance with the Declaration of Helsinki (as revised in 2013). The study was approved by the Ethics Committee of Nanjing Drum Tower Hospital (No. 2020-024) and informed consent was taken from all the patients.

References

1. Loibl S, Poortmans P, Morrow M, et al. Breast cancer. Lancet 2021;397:1750-69.
2. Sung H, Ferlay J, Siegel RL, et al. Global Cancer Statistics 2020: GLOBOCAN Estimates of Incidence and Mortality Worldwide for 36 Cancers in 185 Countries. CA Cancer J Clin 2021;71:209-49.
3. Burstein HJ, Curigliano G, Loibl S, et al. Estimating the benefits of therapy for early-stage breast cancer: the St. Gallen International Consensus Guidelines for the primary therapy of early breast cancer 2019. Ann Oncol 2019;30:1541-57.
4. Litière S, Werutsky G, Fentiman IS, et al. Breast conserving therapy versus mastectomy for stage I-II breast cancer: 20 year follow-up of the EORTC 10801 phase 3 randomised trial. Lancet Oncol 2012;13:412-9.
5. Moran MS, Schnitt SJ, Giuliano AE, et al. Society of Surgical Oncology-American Society for Radiation Oncology consensus guideline on margins for breast-conserving surgery with whole-breast irradiation in stages I and II invasive breast cancer. Int J Radiat Oncol Biol Phys 2014;88:553-64.
6. Tung NM, Boughey JC, Pierce LJ, et al. Management of Hereditary Breast Cancer: American Society of Clinical Oncology, American Society for Radiation Oncology, and Society of Surgical Oncology Guideline. J Clin Oncol 2020;38:2080-106.
7. Atallah I, Milet C, Henry M, et al. Near-infrared fluorescence imaging-guided surgery improves recurrence-free survival rate in novel orthotopic animal model of head and neck squamous cell carcinoma. Head Neck 2016;38 Suppl 1:E246-55.
8. Osako T, Nishimura R, Nishiyama Y, et al. Efficacy of intraoperative entire-circumferential frozen section analysis of lumpectomy margins during breast-conserving surgery for breast cancer. Int J Clin Oncol 2015;20:1093-101.
9. Garcia MT, Mota BS, Cardoso N, et al. Accuracy of frozen section in intraoperative margin assessment for breast-conserving surgery: A systematic review and meta-analysis.

PLoS One 2021;16:e0248768.
10. St John ER, Al-Khudairi R, Ashrafian H, et al. Diagnostic Accuracy of Intraoperative Techniques for Margin Assessment in Breast Cancer Surgery: A Meta-analysis. Ann Surg 2017;265:300-10.
11. Pradipta AR, Tanei T, Morimoto K, et al. Emerging Technologies for Real-Time Intraoperative Margin Assessment in Future Breast-Conserving Surgery. Adv Sci (Weinh) 2020;7:1901519.
12. Lauwerends LJ, van Driel PBAA, Baatenburg de Jong RJ, et al. Real-time fluorescence imaging in intraoperative decision making for cancer surgery. Lancet Oncol 2021;22:e186-95.
13. Hu Z, Fang C, Li B, et al. First-in-human liver-tumour surgery guided by multispectral fluorescence imaging in the visible and near-infrared-I/II windows. Nat Biomed Eng 2020;4:259-71.
14. Gregor A, Sata Y, Hiraishi Y, et al. Preclinical feasibility of bronchoscopic fluorescence-guided lung sentinel lymph node mapping. J Thorac Cardiovasc Surg 2023;165:337-350.e2.
15. Egloff-Juras C, Bezdetnaya L, Dolivet G, et al. NIR fluorescence-guided tumor surgery: new strategies for the use of indocyanine green. Int J Nanomedicine 2019;14:7823-38.
16. Chen QY, Xie JW, Zhong Q, et al. Safety and Efficacy of Indocyanine Green Tracer-Guided Lymph Node Dissection During Laparoscopic Radical Gastrectomy in Patients With Gastric Cancer: A Randomized Clinical Trial. JAMA Surg 2020;155:300-11.
17. Bargon CA, Huibers A, Young-Afat DA, et al. Sentinel Lymph Node Mapping in Breast Cancer Patients Through Fluorescent Imaging Using Indocyanine Green: The INFLUENCE Trial. Ann Surg 2022;276:913-20.
18. Wu S, Li P, Zhang Q, et al. A new fluorescenttargeting tracer contrasts dual tracers in sentinel lymph node biopsy of breast cancer. Future Oncol 2024;20:951-8.
19. Wang G, Luo Y, Qi W, et al. Determination of surgical margins in laparoscopic parenchyma-sparing hepatectomy of neuroendocrine tumors liver metastases using indocyanine green fluorescence imaging. Surg Endosc 2022;36:4408-16.
20. Zhang C, Lin H, Fu R, et al. Application of indocyanine green fluorescence for precision sublobar resection. Thorac Cancer 2019;10:624-30.
21. Ou C, Luo Y, He L, et al. Application of fluorescence endoscopy with methylene blue dye and indocyanine green dual-tracer method in sentinel lymph node biopsy for women with breast cancer. Gland Surg 2023;12:780-90.
22. Sun YS, Zhao Z, Yang ZN, et al. Risk Factors and Preventions of Breast Cancer. Int J Biol Sci 2017;13:1387-97.
23. Sikkenk DJ, Sterkenburg AJ, Burghgraef TA, et al. Robot-assisted fluorescent sentinel lymph node identification in early-stage colon cancer. Surg Endosc 2023;37:8394-403.
24. Vasilyeva E, Nichol A, Bakos B, et al. Breast conserving surgery combined with radiation therapy offers improved survival over mastectomy in early-stage breast cancer. Am J Surg 2024;231:70-3.
25. Agarwal S, Pappas L, Neumayer L, et al. Effect of breast conservation therapy vs mastectomy on disease-specific survival for early-stage breast cancer. JAMA Surg 2014;149:267-74.
26. Bundred JR, Michael S, Stuart B, et al. Margin status and survival outcomes after breast cancer conservation surgery: prospectively registered systematic review and meta-analysis. BMJ 2022;378:e070346.
27. Heidkamp J, Scholte M, Rosman C, et al. Novel imaging techniques for intraoperative margin assessment in surgical oncology: A systematic review. Int J Cancer 2021;149:635-45.
28. Luo J, Chen F, Cao H, et al. Customised 3D-Printed Surgical Guide for Breast-Conserving Surgery after Neoadjuvant Chemotherapy and Its Clinical Application. Bioengineering (Basel) 2023;10:1296.
29. Miyamoto H. Intraoperative pathology consultation during urological surgery: Impact on final margin status and pitfalls of frozen section diagnosis. Pathol Int 2021;71:567-80.
30. Cao Y, Wang P, Wang Z, et al. A pilot study of near-infrared fluorescence guided surgery for primary tumor localization and lymph node mapping in colorectal cancer. Ann Transl Med 2021;9:1342.
31. Borlan R, Focsan M, Maniu D, et al. Interventional NIR Fluorescence Imaging of Cancer: Review on Next Generation of Dye-Loaded Protein-Based Nanoparticles for Real-Time Feedback During Cancer Surgery. Int J Nanomedicine 2021;16:2147-71.
32. Spinoglio G, Bertani E, Borin S, et al. Green indocyanine fluorescence in robotic abdominal surgery. Updates Surg 2018;70:375-9.
33. Sekine Y, Itoh T, Toyoda T, et al. Precise Anatomical Sublobar Resection Using a 3D Medical Image Analyzer and Fluorescence-Guided Surgery With Transbronchial Instillation of Indocyanine Green. Semin Thorac Cardiovasc Surg 2019;31:595-602.

34. Keating J, Tchou J, Okusanya O, et al. Identification of breast cancer margins using intraoperative near-infrared imaging. J Surg Oncol 2016;113:508-14.
35. Pop FC, Veys I, Vankerckhove S, et al. Absence of residual fluorescence in the surgical bed at near-infrared fluorescence imaging predicts negative margins at final pathology in patients treated with breast-conserving surgery for breast cancer. Eur J Surg Oncol 2021;47:269-75.
36. Wang J, Wang W, Chen X, et al. Laparoscopic versus open hepatectomy for intrahepatic cholangiocarcinoma in patients aged 60 and older: a retrospective cohort study. World J Surg Oncol 2022;20:396.
37. Verras GI, Tchabashvili L, Mulita F, et al. Micropapillary Breast Carcinoma: From Molecular Pathogenesis to Prognosis. Breast Cancer (Dove Med Press) 2022;14:41-61.
38. Akrida I, Mulita F. The clinical significance of HER2 expression in DCIS. Med Oncol 2022;40:16.
39. DO J, Chu J, Ahn J, et al. Assessing Resection Margin Status in Breast-conserving Surgery Specimens: Comparison Among Gross Evaluation, Frozen Section Analysis, and Permanent Section Diagnosis in 725 Patients With Breast Cancer. Anticancer Res 2022;42:4453-60.
40. Li W, Zheng Y, Wu H, et al. Breast-conserving therapy versus mastectomy for breast cancer: a ten-year follow-up single-center real-world study. Gland Surg 2022;11:1148-65.

Cite this article as: Yu H, Yao Y, Zhu T, Sun Y, Zhang M, Zhang Y, Cao M, Zhang W, Yao Y. The potential of indocyanine green fluorescence detection in surgical cut margin of breast conserving surgery. Gland Surg 2024;13(6):1031-1044. doi: 10.21037/gs-24-195